

Petrography, geochemistry and geodynamic environment of potassic alkaline rocks in Eslamy peninsula, northwest of Iran

B HAJALILOU^{1,*}, M MOAYYED^{2,**} and GH HOSSEINZADEH²

¹*Department of Geology, Payame Noor University, Tabriz, Iran.*

²*Department of Geology, University of Tabriz, Tabriz, Iran.*

* e-mail: hajalilou@pnu.ac.ir bhshnaha@yahoo.com

** e-mail: m.moayyed@tabriziu.ac.ir

Eslamy peninsula, 360 km² in area, is located in the eastern coast of Urmieh lake in the northwest of Iran. This peninsula is a complex stratovolcano with a collapsed center, which is elevated due to later intrusions of sub-volcanic masses with trachytic to microsyenitic composition. The composite cone consists of a sequence of leucite tephrite, tephrite, leucite basanite, basanite and related pyroclastic rocks. Magmatic activities in the Eslamy peninsula begin with potassic alkaline to ultrapotassic and basic, silica-undersaturated shoshonitic rocks and they are followed by intrusions of lamprophyric dykes and end with acidic magmatism including trachytic, microsyenitic, syenitic and phonolitic domes. The original magma of the Eslamy peninsula rocks has a potassic alkaline nature (Roman type) rich in LREE and LILE and depleted of HREE. These characteristics suggest that the origin of magma can be from deep mantle with a garnet lherzolite composition, a low partial melting rate which has been contaminated by crustal materials in its way up. Fractional crystallization of olivine, diopsidic clinopyroxene and leucite played an important role in the evolution of magmas. Scrutinizing the geodynamic environment of Eslamy peninsula rocks in discrimination diagrams indicates that these rocks must have been formed in a post-collision magmatic arc setting.

1. Introduction

Potassic igneous rocks are categorized as K-rich calc-alkaline rocks, subduction-related shoshonites, within-plate potassic rocks, orogenic ultrapotassic rocks, shoshonitic and alkaline lamprophyres (Morrison 1980; Muller and Groves 1997). K₂O/Na₂O molar ratio in potassic rocks is equal to 1 or a little more and their MgO content is over than 3% (Peccerillo 1992; Foley *et al* 1987). Ultrapotassic rocks have a K₂O/Na₂O molar ratio greater than 2, with the amount of MgO being lower than 3% (Foley *et al* 1987). Nevertheless, the term potassic is usually used for both potassic and ultrapotassic rocks. These rocks are classified into four main groups namely,

lamproites, shoshonites and Roman-type potassic, kamaufigites, and ultrapotassic rocks.

The following hypothesis have been put forward regarding the petrogenesis of these rocks:

- Assimilation of carbonate rocks by basic magma (Rittman 1933; Peccerillo 1992).
- Local infiltration (Harris 1957).
- Zone melting (Key and Gast 1973).
- Mantle metasomatism (Menzies and Hawkes 1981; Peccerillo 1992; Roy *et al* 2004).

In general, it is believed that potassic magmas can not be produced by partial melting of the mantle alone and the other factors like inhomogeneous mantle sources metasomatically rich in LILE and LREE are required as well (Peccerillo 1992;

Keywords. Mineralogy; petrology; geochemistry; volcanology; geodynamics; Eslamy peninsula; Iran.

Foley *et al* 1987). Peccerillo (1992) believes that the volatiles, LILEs and LREEs are accumulated in hydrous minerals such as phlogopite and apatite that are found in the glimmeritic veins and layers beneath the continental crust in the upper mantle.

Shoshonitic and ultrapotassic magmatism in the Eslamy peninsula with the Pliocene (6.5–8 Ma) age has been reported to occur in the eastern coast of the Urmieh lake (Moin-Vaziri *et al* 1991; Moradian 1997, 2007). Several assumptions have been made with regard to the petrogenesis of these rocks, some of which are as follows:

- Final stages of magmatism in the active continental margin due to subduction of Neo-Tethys oceanic crust beneath the central Iran block (Moin-Vaziri 1985; Moin-Vaziri *et al* 1991).
- Magmatism related to continental rift setting (Amidi 1975; Emami 1981; Amidi *et al* 1984).
- Hot spot-related magmatism within a continental crust (Berberian 1981; Berberian and Berberian 1981).

The evidence discussed in this study indicates that magmatism in the Eslamy peninsula must have occurred in a post-collisional magmatic arc.

2. Geological setting

Eslamy peninsula is located in the eastern coast of Urmieh lake (figure 1). This peninsula includes a complex stratovolcano with gentle slope flanks and a collapsed caldera in the central part (Hajalilou and Moayyed 2005). Later intrusion of sub-volcanic trachytic to microsyenitic rocks is supposed to have caused doming and an uplift in the central parts in these sections (figure 2). These rocks are a part of the Tertiary–Quaternary magmatic zone in northwest of Iran. The Eslamy peninsula highlands have their own distinct morphotectonic features, and are separated from the Sahand volcanic rocks by a plain. The gravitational field in this area varies from –110 to –100 milligals and the thickness of the crust is about 42–43 km (Dehghani and Makris 1983).

The Eslamy peninsula's two main faults trending NNW-SSE and ENE-WSW intersect one another almost in the middle space (figure 2). Furthermore, aerial magnetometry data delineates an important lineament trending NNE–SSW in the basal rocks of the peninsula. This lineament is presumably an extension of either the Arax or the Apsheron–Palmira fault extended towards the western coast of the Caspian Sea. The lineament seems to have an important role in the tectonic evolution of the study area.

The Eslamy peninsula stratovolcano is composed of a sequence of leucite basanite to leucite

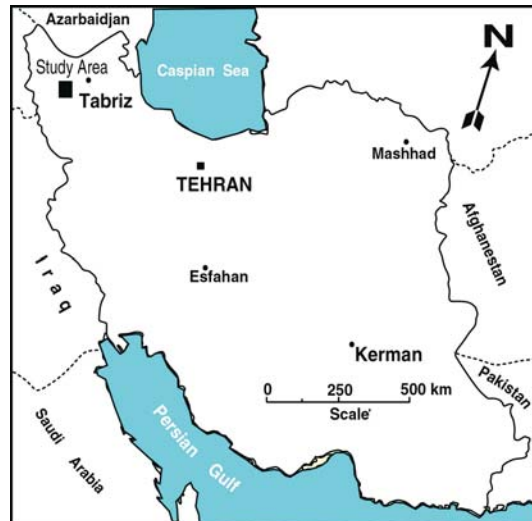


Figure 1. Location of Eslamy peninsula in Iran.

tephrite lavas and the related pyroclastic rocks (breccia and agglomerate). These rocks are cut off by later dykes with composition of basanite and tephrite (figure 3a). The orientation of these dykes is WNW-ESE (figure 2) which implies the extensional mechanism of faults and fractures during later magmatic events of the peninsula. These events have led to the uplifting of the older volcanic units (Hajalilou 2005, 2006). Trachytic to microsyenitic plugs and lamprophyric dykes intersect Pliocene volcanoclastic conglomerate (figure 3b).

3. Petrography

The igneous rocks from the Eslamy peninsula are composed of tephrite, basanite, lamprophyre, trachyte, syenite and ultramafic xenoliths, each of which is taken up separately in some detail below.

3.1 Tephrites

Tephrites exhibit a porphyritic texture and their distinct phenocrysts are clinopyroxene and leucite. The major minerals of these rocks include euhedral to subhedral clinopyroxene (figure 4a) and idiomorphic crystals of leucite. The chemical composition of clinopyroxenes was identified as diopside to salite ($\text{Wo}_{47} \text{En}_{48.5} \text{Fs}_{4.5}$ to $\text{Wo}_{49.3} \text{En}_{36} \text{Fs}_{14.7}$) by EMPA analysis (Moradian 1997). The analyses indicated that the amounts of MgO and CaO get reduced from center to margin in zonal diopside phenocrysts, followed by an increase in the amounts of FeO , Na_2O , Al_2O_3 , TiO_2 and SiO_2 are increasing. In all diopside phenocrysts the increase of Al_2O_3 and TiO_2 is accompanied by a decrease in SiO_2 (Moradian 1997). These crystals show sieve texture

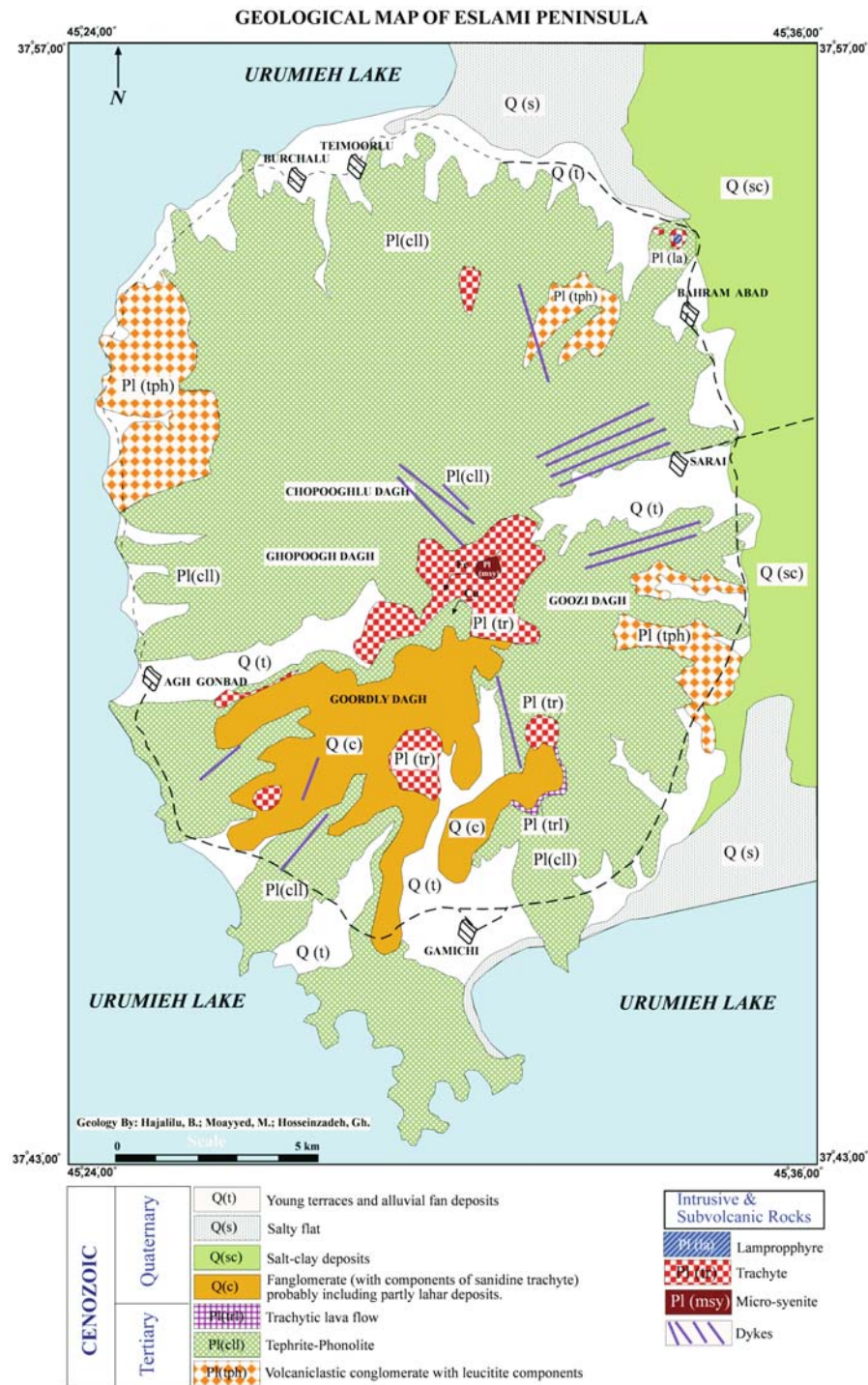


Figure 2. Geological map of Eslamy peninsula.

(figure 4a). Modal data of the Eslamy peninsula igneous rocks is summarized in table 1.

Leucites are the second most important minerals in tephrites and are seen as euhedral crystals of complex twinning with small needles of apatite and rutile within them. This mineral is altered to analcime and orthoclase. These crystals are low in Na_2O ; however, the margins of phenocrysts are rich in Na_2O which might as a

result of an alteration to nepheline and analcime from the margins of these phenocrysts. The Si/Al ratio in phenocryst samples varies from 2.03 to 2.06 (Moradian 1997). Minor minerals of these rocks include fewer amounts of plagioclase, sanidine, olivine, biotite, apatite and opaque minerals which are located in hyaline matrix.

Abundance of clinopyroxene and leucite coupled with the lack of hydrous minerals and plagioclase

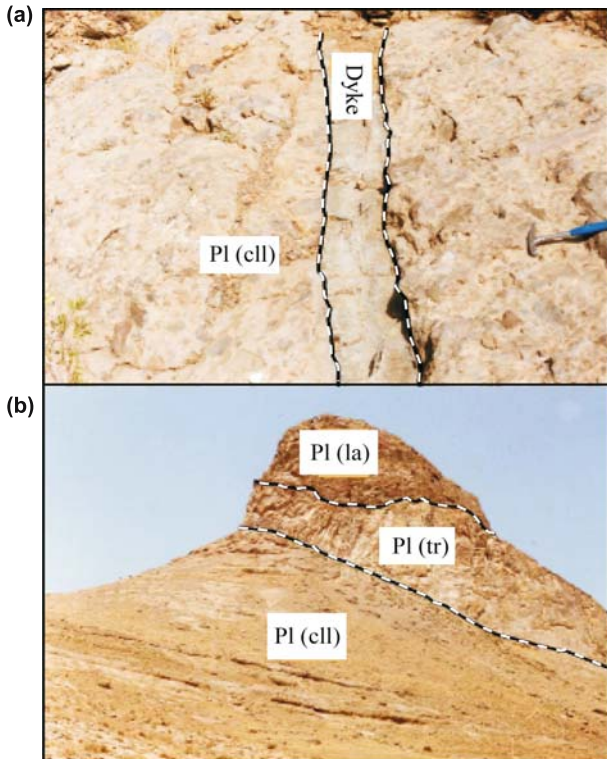


Figure 3. (a) Tephritic-phonolitic dyke intersects volcanoclastic conglomerate. (b) Trachytic plug with lamprophyric head intersects volcanoclastic conglomerate.

show that the crystallization of magma has happened in dry and imbalanced conditions. These rocks basically display hyaloporphyrhetic to hyalomicrolitic porphyry texture.

3.2 Basanites

Basanites mainly consist of euhedral to subhedral clinopyroxene (figure 4b) with the composition varying from diopside to salite ($Wo_{47.5} En_{49.5} Fs_3$ to $Wo_{49.2} En_{41} Fs_{9.8}$) which exhibit sieve texture and normal zoning. Another major mineral of these lavas is euhedral crystals of leucite with a complex twinning. The third most common mineral of basanites is euhedral olivine (figure 4b) with modal amount of 10% to 15%. The composition of these crystals ranges from Fo_{84} to $Fo_{84.8}$ and do not show any interaction margin. The presence of CaO is higher than 0.1% and amount of TiO_2 , Al_2O_3 , Cr_2O_3 and Ni is less than that. The diffusion coefficient of Mg and Fe elements in olivine crystals in relation to matrix is 4% which refers to crystallization of these crystals in high pressure (Moradian 1997). These crystals are basically iddingsitised along crystalline fractures. Minor minerals of basanites are sanidine and magnetite (Hajalilou 2005). Some inclusions of rutile and apatite needles can be seen in leucite. Texture of these rocks is hyaloporphyrhetic to hyalomicrolitic porphyry.

3.3 Lamprophyric dykes

Lamprophyric dykes cut the volcanic rocks (tephrites and basanites) and the related pyroclastics with a NW-SE trend and lie beneath trachyte lavas. These rocks are characterized with euhedral and shiny phenocrysts of mica which can grow up to 3 or 4 cm and show porphyritic texture. The major minerals are euhedral to subhedral phenocrysts of zonal mica (figure 4c) which are delimited in a fine grain matrix of alkali feldspar with ocellar texture and fine grain alteration products. Euhedral to subhedral clinopyroxenes are pseudomorphed by the alteration products (calcite and opaque minerals). Minor minerals consist of amorphous apatite phenocrysts (figure 4c) and opaque minerals like pyrrhotite and magnetite. The biotites composition of these dykes is phlogopite (Moayyed et al 2008).

Spider diagrams pattern for the phlogopite is similar to the pattern for the whole rock but Rh , Ti , K , and Ba contents in the phlogopite are higher than the entire rock and Zr , Nd , P , Sr , Ce , La , Nb and Th contents are lower than those for the whole rock (Moayyed et al 2008).

3.4 Trachytes

Trachytes in the Eslamy peninsula are exposed in three main forms: lava, dyke and subvolcanic domes. Porphyritic texture and sanidine megacrysts which, in some cases, may be as long as 5 cm can be seen in the samples belonging to dykes and subvolcanic domes. Major minerals include sanidine (figure 4d). The minor minerals are subhedral crystals of clinopyroxene, mica, sphene, apatite and the rarest is plagioclase. Megacrysts of sanidine arranged along the flow direction are present in the samples showing microlitic porphyry texture. The composition of sanidine in these rocks is $Or_{62.8}$ to $Or_{72.9}$, and they contain 0–0.15% TiO_2 , 0–1.77% MgO and 0–1.99% FeO . As SiO_2 increases in sanidine crystals, the amount of K_2O grows larger in accordance with it (Moradian 1997). In trachyte lavas, biotite crystals are recognized by TiO_2 and FeO assembly in their margins and their $Mg/Mg + Fe^{+2}$ ratio is less than 0.67 (Moradian 1977). The absence of amphiboles in trachyte lava is a sign of magma crystallization in dry situations. The textures of trachyte lavas are trachytic, felsitic and intergranular. In the samples, belonging to dykes and subvolcanic domes, the main texture is microlitic porphyry.

3.5 Syenites

Syenite to microsyenite masses of Eslamy peninsula, located in the center of this area, are injected

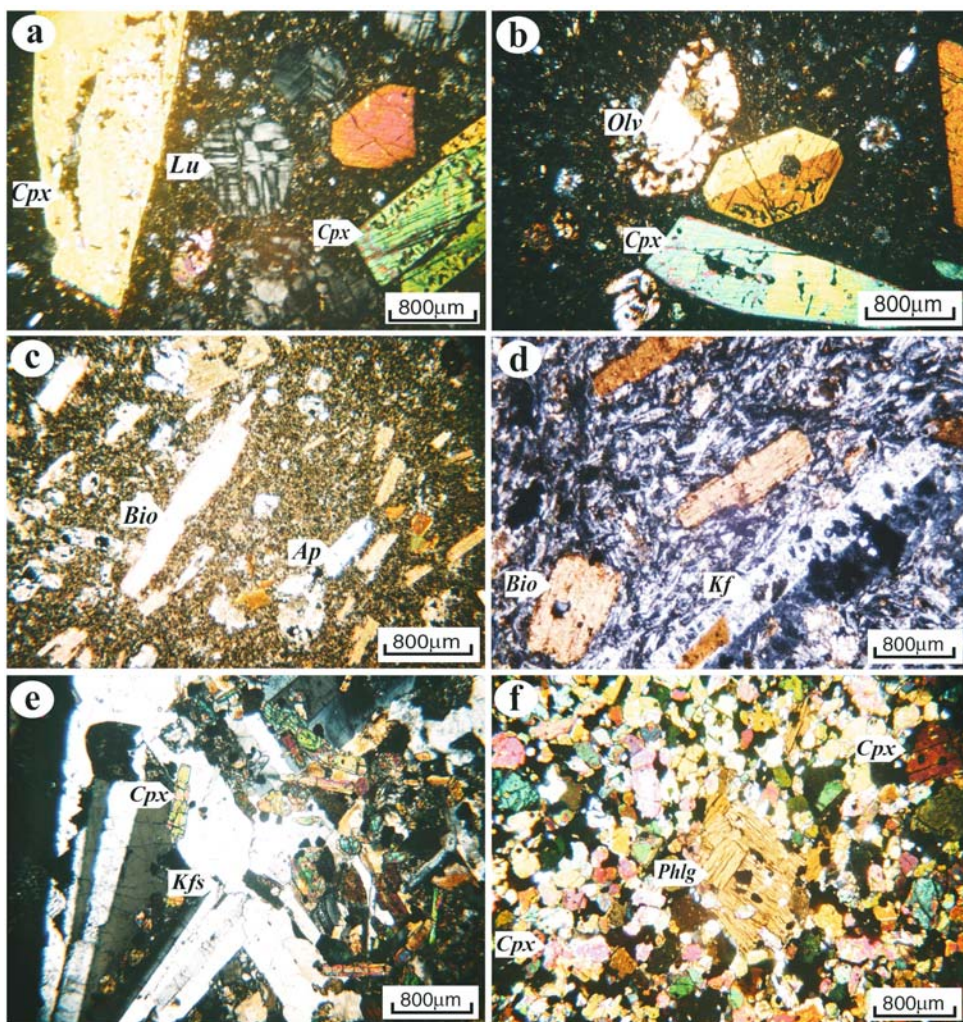


Figure 4. (a) Subhedral clinopyroxene with sieve texture and idiomorphic leucite with complex twinning in tephrites; (b) Euhedral clinopyroxene and olivine in basanite; (c) Subhedral phenocrysts of biotite and apatite in lamprophyric dykes; (d) Phenocrysts of sanidine and trachytic texture in trachyte; (e) Alkalifeldspar and clinopyroxene in syenite; (f) Phenocryst of phlogopite with clinopyroxene in mica clinopyroxenite (mantle xenoliths).

Table 1. *Modal composition from the Eslamy peninsula igneous rocks.*

Rocks	Minerals					
	CPX	Oli.	Lu.	AFs.	Plg.	Bio.
Trachyte	+	-	-	+	+	+
Syenite	+	-	-	+	-	+
Lamprophyre	+	-	-	+	-	+
Basanite	+	+	+	+	+	-
Tephrite	+	-	+	+	+	+

into volcanic and pyroclastic rocks (tephrites, basanites and tuffs) and to the related pyroclastics. The major minerals are subhedral phenocrysts of alkali feldspar and clinopyroxenes, biotite (figure 4e), sphen, apatite and opaque minerals are minor ones. The dominant texture of the mass is granular to trachytoide.

3.6 Clinopyroxenites with mica (ultramafic xenoliths)

These xenoliths can be seen in leucite tephrite to leucite basanite dykes and lavas as circular to ellipsoidal forms. Their color in hand specimen is olive to dark green. The major minerals in these rocks are euhedral to subhedral clinopyroxene, phlogopite and opaque (figure 4f). Phlogopite shows kink banding. These rocks must have originated as mantle xenoliths.

4. Analytical methods

Thirtyone specimens of various rock types were chosen to be analyzed for petrochemical and geodynamic studies. These specimens were sent to the Kansaran Binalood Company for XRF analysis (table 2). A Phillips PW-1480 X-Ray fluorescence

Table 2. Chemical composition of the Eslamy peninsula rocks.

Sample	Teph.1	Teph.2	Teph.3	Teph.4	Teph.5	Teph.6	Teph.7	Teph.8	Teph.9	*Teph.10	*Teph.11	*Teph.12	*Teph.13	*Teph.14
Major elements (wt%)														
SiO ₂	45.86	47.81	48.61	47.97	48.74	49.51	50.21	48.61	50.63	47.81	48.61	47.94	49.01	47.01
Al ₂ O ₃	12.94	12.87	13.6	13.63	12.13	14.11	14.76	11.25	15.23	12.8	13.57	12.77	13.01	12.34
Fe ₂ O ₃ ^t	10.5	9.19	8.96	8.73	9.17	10.67	9.05	8.83	8.22	9.26	8.98	8.96	9.7	10.14
CaO	12.9	11.79	10.74	11.51	11.81	12.01	10.33	11.52	10.37	11.8	10.82	11.8	11.98	10.94
Na ₂ O	1.05	0.74	1.2	2.32	1.13	3.07	2.08	1.31	2.49	0.72	1.18	0.7	2.89	1.08
K ₂ O	4.83	6.43	7.38	5.95	4.86	1.65	5.92	6.38	4.87	6.44	7.42	6.54	5.98	6.48
MgO	5.48	6.07	4.11	5.01	1	3.62	3.18	7.34	4.61	6.17	4.28	6.18	5.31	6.52
MnO	0.16	0.16	0.14	0.146	0.148	0.165	0.152	0.138	0.14	0.16	0.15	0.16	0.18	0.27
TiO ₂	1.51	1.15	1.19	1.02	1.2	1.12	1.06	1.07	1.08	1.15	1.24	1.12	1.08	1.21
P ₂ O ₅	1.66	1.22	1.28	1.38	1.6	1.08	1.012	1.076	0.997	1.24	1.28	1.32	1.21	1.51
Total	96.89	97.43	97.21	97.666	91.788	97.025	97.754	97.544	98.637	97.55	97.53	97.49	100.35	97.5
Minor elements (ppm)														
Y	24	29	29	24	49	36	27	24	20	20	28	30	28	25
Nb	27	35	31	29	39	23	29	20	28	34	32	35	27	30
Ta	1.98	1.8	2.46	2.46	1.73	1.73	1.1	1.86	1.98	1.99	1.98	2.08	1.96	1.96
Ba	3694	2500	4100	2851	2890	2810	2803	3280	4230	1981	3560	1978	2810	2828
W	10	57.4	84.7	64	48.6	28	36	130	165	64	44	18	12	10
Pb	41	39	35	41	35	46	28	28	48	38	36	32	28	29
La	55	96.64	90.62	62	87.88	77	55	69.2	110.7	82	66	85	78	52
Ce	82	154	151	88	157	122	112	117	173	142	112	148	132	112
Th	11	36.6	27.04	14	38.11	20	21	21.37	31.67	21	17	20	19	29
U	1	3.23	3.17	4	3.68	3	6	6.06	7.31	2	3	2	3	8
Mo	7	4.3	2.3	7	2.8	6	8	3.5	3	6	4	6	6	4
S	5	5	6	7	5	7	10	6	2	6	8	7	8	11
Cl	197	165	169	836	233	91	231	347	1318	160	168	164	91	189
V	193	175	150	181	179	201	161	132	142	174	152	176	189	301
Cr	50	248	90.6	49	35.2	5	19	534	91.6	84	32	82	54	22
Co	24	40.22	37.29	21	35.59	27	19	44.71	36.45	19	18	17	27	23
Ni	39	52	21	31	41	15	22	90	29	54	32	59	48	52
Cu	153	109	83	100	86	30	82	42	35	110	85	108	58	216
Zn	70	66	95.4	63	65	81	65	64	102	75	62	54	64	84
Rb	108	303	279	123	651	276	163	205	96	192	186	188	212	154
Sr	820	1020	1160	885	925	1151	1006	701	1640	742	910	752	882	841
Zr	238	250	214	257	334	262	234	422	278	260	298	294	284	218
Sb	1	0.16	1	1	0.41	1	1	0.25	0.34	1	1	1	1	1
Sn	1	1	2	2	1	3	1	4	1	1	2	1	3	1
Cd											8	9	2	3
Bi											1	1	1	2

	1	1	1	1	1	1	1	1	1	1	1	1	1	1	1		
Ag	1	78	63	36	92	93	71	53	51	79	64	78	83	43	1		
Nd	67	1.56	1.13	4	4.26	34	19	2.26	14.31	17	26	12	18	28			
As	39	14	12	15	15	13	15	10	14	12	13	12	13	14			
Ga																	
Yb	3.65	2.45	2.45	2.67	11.38	11.38	11.38	1.82	3.64	3.64	2.67	3.68	3.59	3.72			
Hf	8.22	10.02	10.02	0.55	0.55	0.55	0.55	7.55	6.33	9	10	9	10	8			
Lu	0.53	0.44	0.44	0.55	0.55	0.55	0.55	0.29	0.39								
Eu	2.88	3.68	3.68	3.42	3.42	3.42	3.42	2.75	3.04								
Tb	2.02	1.64	1.64	1.75	1.75	1.75	1.75	1.72	1.62								
Sm	13.2	11.96	11.96	16.01	16.01	16.01	16.01	11.31	11.38								
Nd	79	90	90	86	86	86	86	85	60								
Sc	38.75	37.19	37.19	21.18	21.18	21.18	21.18	40.39	31.41								
Cs	16.58	16.71	16.71	47.47	47.47	47.47	47.47	11.64	9.04								
Sample	Sy.1	Sy.2	Sy.3	Sy.4	*Sy.5	*Sy.6	*Sy.7	*Sy.8	*Sy.9	Lamp.1	Lamp.2	Lamp.3	Lamp.4	Lamp.5	Lamp.6	Lamp.7	Lamp.8
Major elements (wt%)																	
SiO ₂	62.42	59.34	56.85	56.54	59.38	61.98	62.4	57.85	63.18	53.13	52.53	38.29	43.04	47.48	42.66	52.93	51.78
Al ₂ O ₃	15.02	15.12	13.86	17.3	15.1	15.02	15.02	13.8	15.08	14.47	13.15	8.88	9.13	12.34	11.13	13.48	13.58
Fe ₂ O ₃ ^t	5.4	4.52	6.68	4.05	4.5	5.44	5.42	5.98	4.08	5.88	7.85	16.05	9.94	13.14	9.58	6.62	6.41
CaO	2.87	6.01	5.65	5.95	6.1	2.88	2.88	5.2	1.88	8.94	8.26	17.35	13.16	9.78	11.81	8.63	9.85
Na ₂ O	2.74	0.9	1.31	0.93	1.26	2.7	2.7	1.82	1.92	0.85	1.68	0.48	0.3	1.03	3	0.7	1.45
K ₂ O	8.71	8.21	8.63	9.42	8.17	8.8	8.71	8.63	9.44	7.84	6.98	2.39	5.49	6.55	6.91	8.04	7.41
MgO	1.2	1.38	3.76	1.46	1.44	1.27	1.22	2.88	0.98	3.83	4.46	10.77	12.78	5.64	6.7	4.34	4.03
MnO	0.07	0.076	0.12	0.07	0.08	0.07	0.07	0.12	0.09	0.097	0.119	0.17	0.12	0.26	0.14	0.107	0.102
TiO ₂	0.776	0.672	0.97	0.57	0.67	0.78	0.78	0.97	0.68	0.85	1.06	1.88	2.17	1.12	1.43	1.14	1.01
P ₂ O ₅	0.29	0.69	0.72	0.56	0.69	0.32	0.32	0.78	0.21	1.05	0.98	3.01	2.18	1.15	1.15	1.11	
Total	99.496	96.918	98.55	96.85	97.39	99.26	99.56	98.03	97.54	96.937	97.069	99.27	98.31	98.49	94.376	97.137	96.732
Minor elements (ppm)																	
Y	30	28	31	23	40	82	30	31	34	26	25	19	22	25	25	27	27
Nb	73	39	39	31	40	68	73	48	57	28	23	5	5	30	28	35	37
Ta																	
Ba	2828	3140	2488	2160	1900	2814	2820	2470	1964	1414	3210	2974	3679	2244	2908	2372	2161
W	97	100	61	108	63	96	97	60	40	61	80.1	37	7	51	2	53	69
Pb	43	59	40	38	60	44	43	40	44	35	53	8	4	18	40	36	38
La	52	80.76	50	80.31	48	53	52	50	54	43	82.4	43	33	68	45	44	45
Ce	112	134	75	126	60	110	112	102	117	99	138	68	64	137	85	77	96
Th	45	56.42	34	38.67	37	44	45	38	40	19	25.16	2	6	21	23	24	30
U	10	14.61	19	12	9	10	10	19	12	10	7.01	1	4	8	9	7	12
Mo	1	5.56	5	3.7	2	1	1	1	1	6	4.8	9	7	8	4	4	4
S	543	9	8	5	9	540	543	82	32	8	51	41	7	11	236	8	8
Cl	846	34	119	66	34	840	840	219	48	137	424	891	260	274	187	300	120
V	86	93	138	74	94	88	88	132	79	114	143	288	164	301	159	126	131

Sample	Sy.1	Sy.2	Sy.3	Sy.4	*Sy.5	*Sy.6	*Sy.7	*Sy.8	*Sy.9	Lamp.1	Lamp.2	Lamp.3	Lamp.4	Lamp.5	Lamp.6	Lamp.7	Lamp.8
Cr	22	121	72	259	30	21	22	38	5	89	37.27	79	59	150	138	82	89
Co	23	20.08	17	32.24	11	24	23	17	6	14	31.11	33	25	28	11	13	19
Ni	20	25	43	17	24	22	20	22	9	24	26	44	95	37	51	28	32
Cu	706	71	385	53	70	704	218	118	10	55	101	10	4	30	84	65	65
Zn	83	46	92	93.9	47	88	83	92	68	51	116	66	49	258	79	56	58
Rb	195	300	255	225	210	198	195	255	288	175	153	46	117	155	195	207	191
Sr	1206	156	1163	895	1288	1214	1207	1162	1218	751	949	450	483	851	531	843	864
Zr	586	637	391	308	437	568	586	432	490	293	317	100	49	208	279	364	364
Sb	1	1.22	1	0.91	1	1	1	1	1	2	0.67	1	1	2	1	1	2
Sn	1	5	3	4	5	1	1	3	3	4	1	1	2	4	3	2	2
Cd					1	BD	1	1	1								
Bi					1	1	1	1	1	1	1	1	1	1	1	1	1
Ag	1	1	1	1	1	1	1	1	1	1	1	1	1	1	1	1	1
Nd	35	62	29	21	63	37	44	31	28	51	46	77	32	35	38	30	44
As	40	3.76	37	8.41	4	42	40	32	28	53	12.69	15	25	55	31	5	31
Ga	18	20	17	19	21	19	18	17	21	13	14	9	9	13	15	15	14
Yb		1.6		2.16	1.6	1.43	2.88	2.58	2.15			3.42					
Hf		13.1		10.4	10	13	24	19	17			8.83					
Lu		0.4		0.22								0.39					
Eu		2.4		2.5								3.1					
Tb		1.32		1.45								1.9					
Sm		9.55		12.8								10.62					
Nd		64		88								96					
Sc		20.23		33.02								29.81					
Cs		4.15		47.43								34.28					

Sample	Tr.1	Tr.2	Tr.3	Tr.4	Tr.5	Tr.6	Tr.7	Tr.8	Tr.9	*Tr.10	*Tr.11	*Tr.12	*Tr.13
Major elements (wt%)													
SiO ₂	64.25	64.92	54.04	60.34	58.4	60.46	63.67	61.79	64.9	56.64	59.3	60.3	61.7
Al ₂ O ₃	16.54	16.9	17.16	15.01	15.3	15.42	14.39	16.5	16.88	18.02	15.12	15.01	15.8
Fe ₂ O ₃ ^t	3.63	2.34	6.01	4.24	5.58	4.63	6.11	4.27	2.34	5.44	4.5	4.14	4.2
CaO	0.65	1.44	6.17	5.04	4.2	4.82	1.66	3.45	1.44	5.58	5.88	5.04	3.58
Na ₂ O	1.88	4.26	0.62	1.96	1.14	2.02	4.37	2.68	4.24	4.62	0.92	1.84	2.7
K ₂ O	10.56	7.74	9.22	8.83	10.32	8.36	6.06	8.4	7.78	7.62	8.12	8.82	8.4
MgO	0.26	0.24	1.07	1.49	1.12	1.17	1.5	0.51	0.23	2.51	1.28	1.18	0.82
MnO	0.086	0.081	0.13	0.088	0.12	0.092	0.07	0.096	0.08	0.12	0.08	0.09	0.1
TiO ₂	0.53	0.268	0.845	0.54	0.85	0.57	0.7	0.5	0.27	0.61	0.67	0.54	0.49
P ₂ O ₅	0.08	0.056	0.4	0.53	0.37	0.46	0.24	0.21	0.06	0.38	0.7	0.53	0.48
Total	98.466	98.245	95.665	98.07	97.4	98.002	98.77	98.406	98.22	101.54	96.57	97.49	98.27

Minor elements (ppm)	32	33	37	32	30	32	25	37	30	20	28	33	34
Y	32	30	29	33	32	32	25	49	74	16	39	47	60
Nb	57	73	64	47	76	55	49	68	74	2.12	2.32	2.41	2.44
Ta	2.67	2.94				3.24	3.51	3.38	3.48				
Ba	2210	1400	3025	1413	3727	2270	2310	2500	968	2308	1980	1490	1850
W	57.1	180	56	129	74	144	100	168	147	7	52	88	92
Pb	69	101	60	42	33	69	112	69	102	47	59	42	62
La	75.53	106	81	48	46	91.65	29.63	109.3	65	28	48	52	65
Ce	125	154	161	99	98	142	114	160	78	27	59	99	128
Th	57.63	109.9	40	49	49	75.76	58.88	99.26	79	44	36	49	67
U	3.7	16.88	33	10	19	10.68	16.37	7.53	15	4	9	10	5
Mo	2.8	5.4	3	2	1	4.1	3.2	4.36	1	2	2	3	1
S	9	8	85	9	8	10	179	11	8	84	12	9	11
Cl	48	1684	175	97	135	34	137	26	1680	175	36	97	26
V	77	44	121	82	107	85	110	69	40	117	92	80	68
Cr	7.5	3.3	3	45	4	75.1	19.4	6.3	2	37	32	28	12
Co	7.18	12.42	13	12	12	19.02	19.02	15.61	9	21	11	10	47
Ni	4	6	9	17	17	8	8	5	6	18	25	17	5
Cu	10	9	111	59	4	28	13	19	9	66	71	50	19
Zn	62	59.8	70	53	77	85.6	65.3	72.7	56	65	46	50	52
Rb	358	254	157	268	224	371	153	323	210	62	228	269	229
Sr	1380	1430	1331	1205	1341	1140	260	1750	1230	988	1280	1208	1218
Zr	395	789	531	557	798	580	537	687	838	534	440	557	688
Sb	0.65	0.66	1	1	1	0.68	1.34	0.71	4	BD	1	1	1
Sn	3	1	2	2	3	4	4	1	BD	BD	5	2	1
Cd									1	1	2	1	2
Bi									1	1	1	1	1
Ag ^G	1	1	1	1	1	1	1	1	1	1	4	2	3
Nd	29	32	41	35	46	48	38	62	32	30	62	35	61
As	24.25	22.86	28	52	13	8.21	20.83	5.75	54	28	3	8	13
Ga	21	28	18	18	18	18	18	20	27	18	20	18	20
Yb	2.15	1.23			2.64	2.46	2.73	2.33	20	21.58	2.46	1.6	2.64
Hf	16.65	23.09			16.94	14.45	14.45	21.58		16	13	17	22
Lu	0.34	0.44			0.45	0.31	0.37						
Eu	2.7	1.37			2.54	1.96	2.5						
Tb	0.82	0.9			1.2	1.33	1.44						
Sm	6.78	7.54			9.45	5.9	9.21						
Nd	42	49			90	48	45						
Sc	5.91	1.72			14.57	12.08	7.56						
Cs	10.71	32			14.22	18.11	31.45						

Teph: Tephrite, Sy: Syenite, Tr: Trachyte, Lamp: Lamprophyre (*: Data from Moayyed *et al.* 2008).

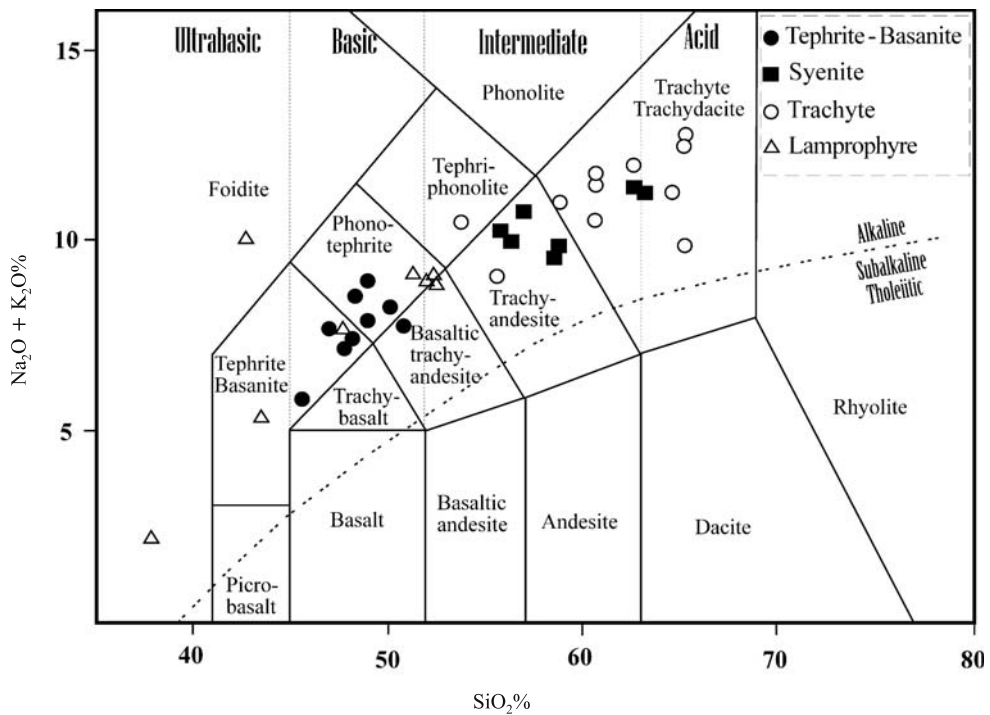


Figure 5. Rock types of Eslamy peninsula in TAS diagram after Le Bas *et al* (1986).

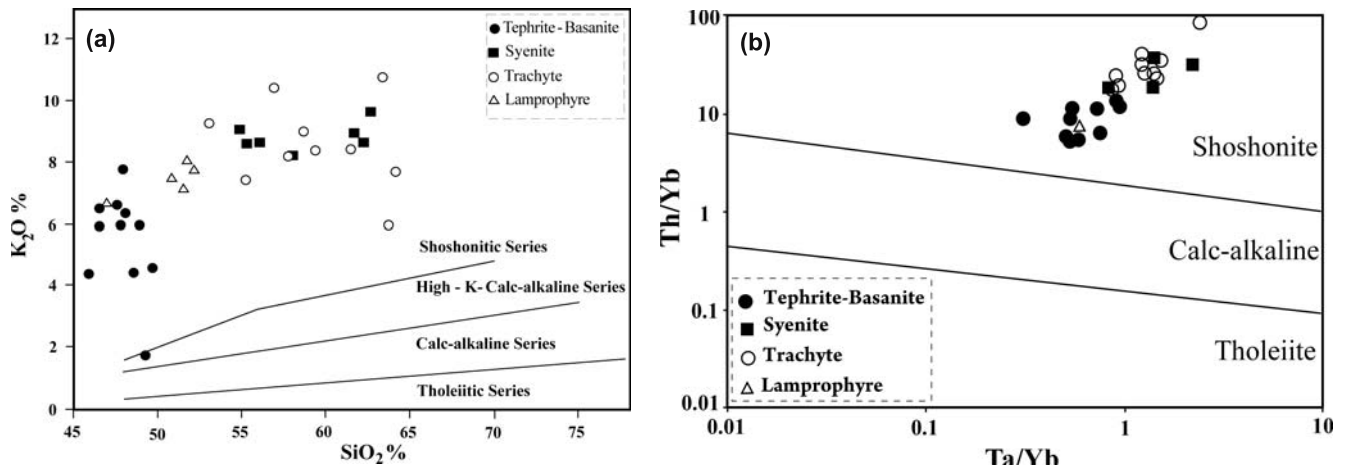


Figure 6. Eslamy peninsula rocks plot in the shoshonite field in diagram of K_2O vs. SiO_2 (after Peccerillo and Taylor 1976) and Th/Nb vs. Ta/Yb (after Pearce 1983).

was used for major and trace element analyses. The amounts of major oxides and 27 elements were determined in these specimens as well. Furthermore, 14 specimens were selected for studying the behaviour of rare earth elements (REE). 33-element analyses were performed using Neutron Activation Analysis (NAA) method. A miniature neutron source reactor (MNSR) operating in 27 kW condition in Isfahan Nuclear Research Center was used for NAA. The error in the analyses was about 1%. In addition to the above-mentioned samples, the results of analyses included 15 samples

(Moayyed *et al* 2008) were used for drawing the graphs and conclusions (table 2).

5. Geochemistry

Based on analytic data and the plot of alkalis *vs.* silica (TAS) of the old volcanism in Eslamy peninsula, the samples lie within the field of basalt, trachy-basalt, tephrite and phonotephrite. Samples representing young magmatic activities were plotted within the trachyte, trachyandesite, phonolite,

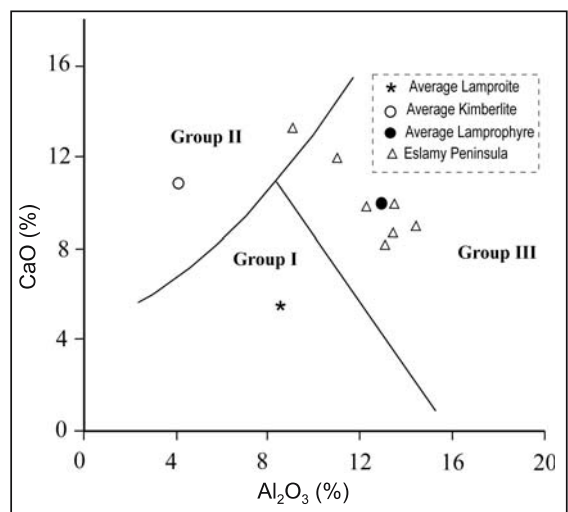


Figure 7. Eslamy rocks plot in the group III of potassic igneous rocks (after Foley *et al* 1987).

trachyphylonolite, syenite and syenodiorite fields and lamprophyre samples were represented in the foidite, tephrite and trachyandesite fields (figure 5).

In general, based on the K_2O/SiO_2 diagram of Peccerillo and Taylor (1976) and the $Th/Yb-Ta/Yb$ diagram of Pearce (1983), the original magma of Eslamy peninsula rocks had a shoshonitic to ultrapotassic nature (figure 6a, b). The K_2O/Na_2O ratio in tephritic and basanitic rocks is always higher than 1, even reaching 4 at times. These rocks have normative olivines and leucites, rich in LILE and LREE. The above-mentioned qualities also exist in trachytes, phonolites, syenites and lamprophyres of the study area. In the CaO/Al_2O_3 diagram of Foley *et al* (1987) the rock types of Eslamy peninsula plot in field III (Roman type rocks, figure 7). Geochemical investigation of minor and trace elements shows these rocks to be rich in LIL. This characteristic is

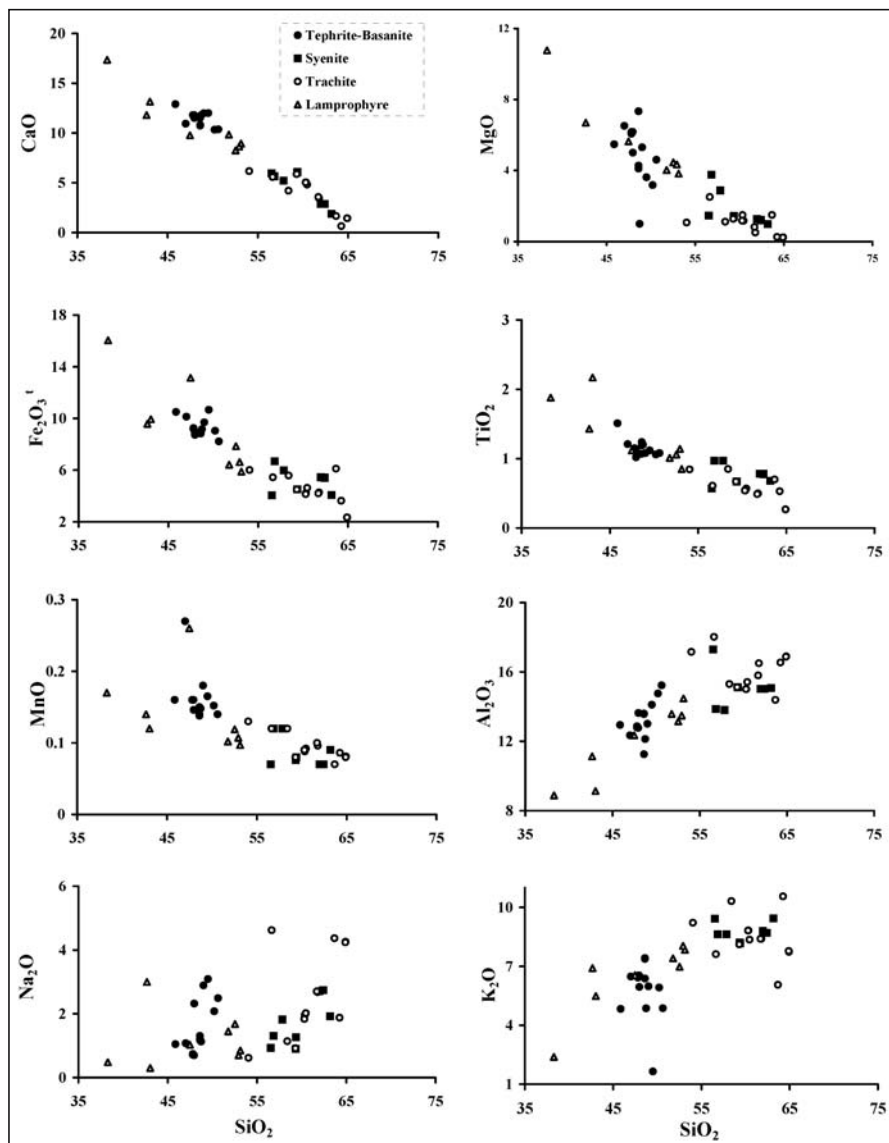


Figure 8. Harker variation diagrams for Eslamy peninsula rocks (after Harker 1909).

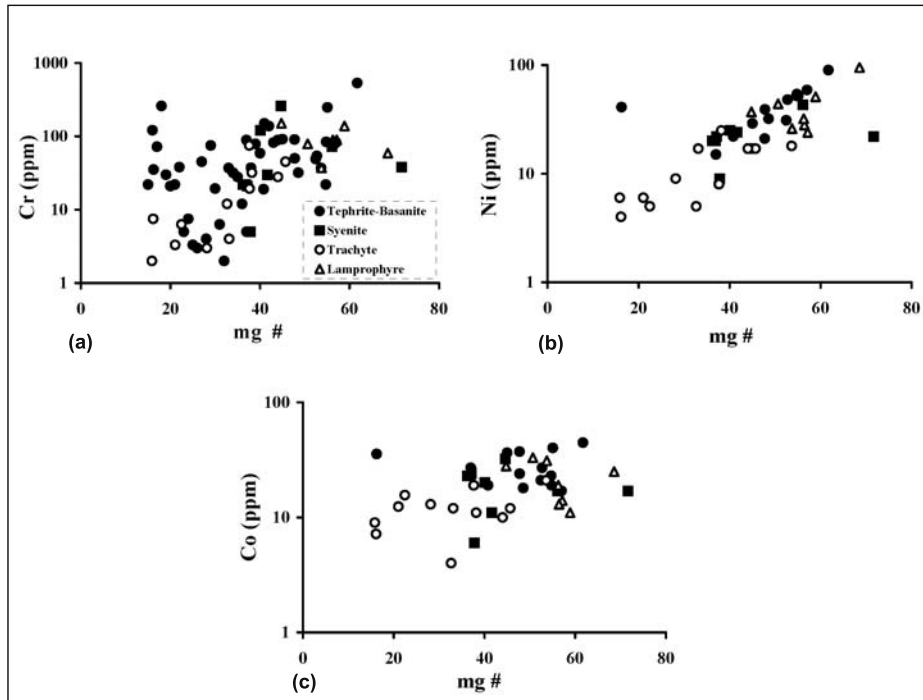


Figure 9. Eslamy peninsula rocks plot in variation diagrams (a) $\text{mg } \#/\text{Cr}$, (b) $\text{mg } \#/\text{Ni}$, and (c) $\text{mg } \#/\text{Co}$.

related to the role of liquid phases in magma generation (Rollinson 1993). Depletion of HFSE is an important feature in Roman type rocks that exist in Eslamy peninsula rocks.

Harker diagram was used for studying the major oxides *vs.* silica variations. Investigation of these diagrams showed that there is a geochemical similarity between all rock types of the peninsula (figure 8).

CaO , MgO , Fe_2O_3 , TiO_2 and MnO decrease with SiO_2 increasing. The similarities between TiO_2 and Fe_2O_3 decline in relation to ilmenite, magnetite and titanomagnetite crystallization. The sharp decline in MgO *vs.* silica (under 50% of silica) show olivine (in early stage) and diopside (in latter stages) crystallization. There is no distinctive variation for K_2O and Na_2O *vs.* silica. This case may indicate crustal contamination in Eslamy peninsula rocks. High amounts of K_2O in mafic rocks reveal that crystallization of leucite has happened in dry conditions. Ca rich plagioclases are absent in Eslamy peninsula rocks so intense decreases in CaO and subsequent increases in Al_2O_3 was in relation to diopside crystallization. The replacement of iron by manganese in olivine and pyroxene caused a slow decrease in MgO *vs.* silica.

The investigation of mg/Ni diagram showed the fractional crystallization of olivine in magma. Dispersion of samples in mg/Cr and mg/Co is responsible for crustal contamination (figure 9).

The ratio of $(\text{Ba/La})_n$ and $(\text{Th/Nb})_n$ in Eslamy peninsula rocks are between 1.29 to 10.95 and 3.35

to 23.06. These characteristics prove the crustal contamination on the petrogenesis of ultrapotassic rocks in Eslamy peninsula (Taylor and McLennan 1985). $\text{Al}_2\text{O}_3/\text{TiO}_2$ ratio in the primitive mantle (PM) is about 27.75, in upper mantle it is 22 and the average of this ratio in Eslamy peninsula is 19.2 (63.1–4.21), so this amount shows crustal contamination of magma that originated from the mantle. Thus the ratio of Zr/Nb and Rb/Sr is about 14.82 and 0.031 in the primitive mantle (PM), but it is 9.09 and 0.123 in the continental crust (Taylor and McLennan 1985). Variations of Zr/Nb and Rb/Sr in Eslamy peninsula ratios are from 6.9 to 33.4 (10.8 average) and 0.06 to 1.92 (0.26 average). The low ratio of Zr/Nb and high ratio of Rb/Sr in relation to primitive mantle, point to the role of continental crust in Eslamy peninsula magmatism.

Scrutinizing the major and trace elements behaviour in the Eslamy peninsula rocks shows that fractional crystallization and segregation of olivine, clinopyroxene and leucite are the main factors controlling the evolution of the magmas. The existence of a large amount of leucite in basanites and tephrites reveals that the corresponding magmas are solidified in low water pressure or even in dry conditions. Probable contamination by crustal rocks and magma mixing were among the other factors in magmatic evolution of the studied rocks. High Nb/Ta and Zr/Hf ratios (Dupuy *et al* 1992; Rudnick *et al* 1993; Furman and Graham 1999; Foley *et al* 2002) in the lamprophyres studied

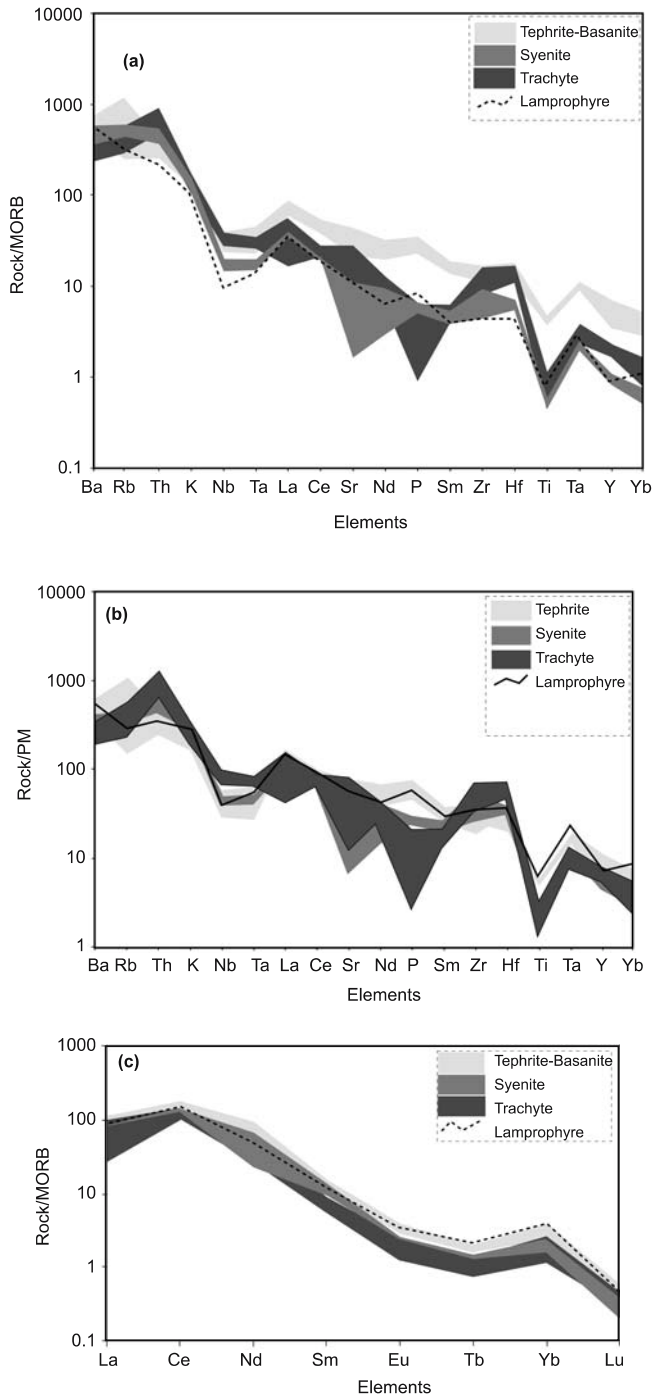


Figure 10. Spider diagrams normalized to the (a) MORB, (b) PM, and (c) REE pattern normalized to MORB (data for MORB and PM from Sun and McDonough 1989).

indicate enrichment process for the source region prior to partial melting and crustal contamination or differential crystallization (Moayyed *et al* 2008). The above-mentioned ratios are controlled by magmatic processes such as partial melting, crystallization and rutile and amphibole metasomatism in the mantle (Ionov *et al* 1997; Foley *et al* 2000, 2002; Tiepolo *et al* 2001). High REE/HFSE ratio for the Eslamy lamprophyres such as high Eu/Ti

may indicate a carbonatitic metasomatism as well. Non-existence of negative anomaly for Eu shows that the mechanism of fractional crystallization and plagioclase separation does not play any significant role in Eslamy peninsula magmatism. High amounts of Th and U in the Eslamy rock units show possible contamination by the middle to upper crust (Taylor and McLennan 1985). To elucidate the nature of the Eslamy peninsula lamprophyres, they are compared with typical alkaline (Spanish Central System) and calc-alkaline lamprophyres (Orejana *et al* 2006).

The study of spider diagrams which were plotted for REE and normalized to MORB and PM indicates that these elements have the same behaviour in basic, intermediate and acidic rocks of the peninsula and display a general negative slope (figure 10a, b, c). This characteristic suggests a co-magmatic origin for the studied rocks and also is demonstrative of great depth and a high CO₂/H₂O ratio. Most of these features are attributed to the origin of these rocks from a metasomatised mantle (Guo *et al* 2004). The absence of amphibole in peninsula rocks can explain the negative anomaly for HREE (Rollinson 1993). The positive anomaly for Th, Rb, K and Ba, is similar to Roman type and may reflect crustal contamination in magma evolution and low ratio melting in enriched mantle (Taylor and McLennan 1985; Wilson 1989; Rollinson 1993).

The negative anomaly for Ta, Nb and Ti can show the role of subducted liquids in mantle metasomatism (Rollinson 1993). The negative anomaly of P in peninsula is an important index for high potassic post collision rocks (Muller and Groves 1997).

6. Geodynamic environment

Tectonic setting of the shoshonitic and ultrapotasssic rocks of the Eslamy peninsula were investigated using the diagram proposed by Muller and Groves (1997) (figure 11) and it was deduced that potassic and ultrapotasssic magmatism of the Eslamy peninsula has occurred in a post-collision magmatic arc (figure 11).

This study shows that, despite the former models for magmatism in the Eslamy peninsula, this geological event is neither related to subduction of Neo-Tethys beneath the central Iranian plate, nor did it occur in a continental rift zone. It could be suggested that the combination of fault displacements and their trend distribution relative to the maximum stress applied to the studied area, had an important role in post-collision magmatism of the Eslamy peninsula. Evidence to

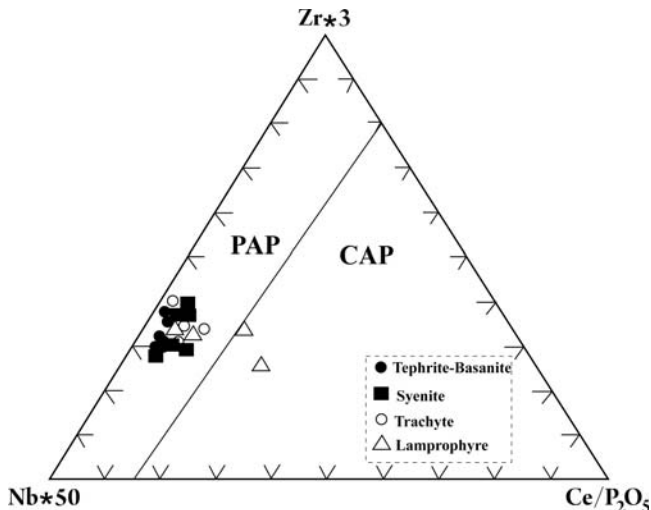


Figure 11. Ce/P₂O₅-Nb*50-Zr*3 diagram for separation of potassic rocks interrelation with post collision arc (PAP) and active continental margin (CAP) after Muller *et al* (1992) with position of Eslamy peninsula rocks.

suggest this can be found in the fact that there are a large number of fault systems in the central Iranian block and in the northwest of Iran and also considering the oblique pressure due to the convergence of the Iranian continental crust and the Arabian plate. The fore-mentioned having been caused by the spreading of the Red Sea.

7. Conclusions

Eslamy peninsula is a complex stratovolcano with a collapsed caldera which is intruded by later lamprophyres, trachytes, phonolites and syenites. The older magmatic activities include tephrite, basanite and the related pyroclastic rocks whereas the younger events tend to be acidic terms.

Sieve texture and normal zoning in clinopyroxenes and the existence of abundant amounts of leucites in tephritic and basanitic lavas demonstrate that magma mixing, assimilation followed by a quick pressure decrease during ascent were the main factors in the evolution of relatively dry magmas of the Eslamy peninsula.

The magmas that produced rocks of the peninsula must have had a shoshonitic to ultrapotassic nature (Roman type) and had most likely been generated from partial melting of garnet lherzolitic mantle with low partial melting ratio in a high CO₂/H₂O condition, probably. Investigation of Harker diagrams showed that there is a geochemical similarity between all rock types of Eslamy peninsula. These magmas are presumed to have been contaminated by crustal materials during rising up toward the surface. Variation of K₂O,

Na₂O vs. silica and mg ≠ /Cr, Co and the ratios of (Ba/La)_n, (Th/Nb)_n, Al₂O₃/TiO₂, Zr/Nb and Rb/Sr show the crustal contamination in Eslamy peninsula rocks. Fractional crystallization of olivine, diopsidic clinopyroxene and leucite played an important role in the evolution of magmas.

Existence of a large amount of leucite in basanites and tephrites reveals that the corresponding magmas are solidified in low water pressure or even dry conditions. High REE/HFSE ratio for the Eslamy lamprophyres such as high Eu/Ti may indicate a carbonatitic metasomatism as well.

Spider diagrams of REEs imply that all rocks in peninsula are co-magmatic and general negative slope along with high LREE and low HREE anomalies suggest for a garnet lherzolite source and partial melting in high CO₂/H₂O conditions. LREE concentrations in the lamprophyre dykes and plugs reflect the existence of garnet as a residue of the melting (Polat *et al* 1997). The negative anomaly for Ta, Nb and Ti can show the role of subducted liquids in mantle metasomatism.

Shoshonitic and ultrapotassic magmatism of Eslamy peninsula is supposed to have occurred in a post-collisional tectonic setting (Muller and Groves 1997) without any relation to Neo-Tethyan subduction or continental rifts.

Acknowledgements

The authors would like to thank the Payame Noor University for financial support. We are thankful to Dr A A Clagari, Dr M Moazzen, M Hoseinpour and M Hajjalilu for their valuable suggestions.

References

- Amidi S M 1975 Contribution à L'étude stratigraphique, Pétrologique, et Pétrochimique des roches magmatiques de la région de Natanz-Nain-Surlc (Iran Central); *The'se Doct. Etat*, Grenoble.
- Amidi S M, Emami M H and Michel R 1984 Alkaline character of Eocene volcanism in the middle part of central Iran and its geodynamic situation; *Geologische Rundschau* **73** 917–932.
- Berberian F 1981 Petrogenesis of Iranian plutons; a study of the Natanz and Bazman intrusive complex; Ph.D. thesis, University of Cambridge, 300p.
- Berberian F and Berberian M 1981 Tectono-plutonic episodes in Iran, in Zagros, Hindukush, Hymalaya, geodynamic evolution. In: (eds) Gupta H and Delany F, *American Geophysical Union, Geodynamics Series* **3** 5–32.
- Dehgani G A and Makris J 1983 The gravity field and crustal structure of Iran. In: Geodynamic project (Geotraverse) in Iran; *Geol. Surv. Iran, Report.* **51** 51–68.
- Dupuy C, Liotard J M and Dostal J 1992 Zr/Hf fractionation in intraplate basaltic rocks: carbonate metasomatism in the mantle source; *Geochim. Acta* **56** 2417–2423.

- Emami M H 1981 Geologie de la regim de Qom-Aran (Iran), Contribution a' l'etude dynamique et geochemique du volcanisme tertiaire de l' Iran central; *These d'Etat*. Univer. Grenoble, France.
- Foley S F, Tiepolo M and Vannucci R 2002 Growth of early continental crust controlled by melting of amphibolite in subduction zones; *Nature* **417** 837–840.
- Foley S F, Barth M G and Jenner G A 2000 Rutile/melt partition coefficient for trace elements and assessment of the influence of rutile on the trace element characteristics on the subduction zone magmas; *Geochim. Cosmochim. Acta* **64** 629–638.
- Foley S F, Venturelli G, Green D H and Toscani L 1987 The ultra-potassic rocks: characteristics, classification and constraints for petrogenetic models; *Earth Sci. Rev.* **24** 81–134.
- Furman T and Graham D 1999 Erosion of lithospheric mantle beneath the east African rift system: Geochemical evidence from the Kivu volcanic province; *Lithos* **98** 237–262.
- Guo F, Fan W, Wang Y and Zhang M 2004 Origin of early cretaceous calc-alkaline lamprophyres from the Sulu orogen in eastern China: Implications for enrichment processes beneath continental collisional belt; *Lithos* **78** 291–305.
- Hajalilou B 2005 Investigation of mineral resources in alkaline rocks from Eslamy peninsula in Urmia lake, 3MA, Morocco.
- Hajalilou B 2006 Metallic and nonmetallic mineralization in shoshonitic rocks, 5th European Congress on Regional Geoscientific Cartography and Earth Information Systems, Barcelona, Spain.
- Hajalilou B and Moayyed M 2005 Petrography and petrology of the alkaline potassic rocks from Eslamy peninsula, NW of Iran and their geodynamic environment, EGU, Austria.
- Harker A 1909 The natural history of igneous rocks. London, Huen, 383 p.
- Harris P G 1957 Zone refining and the origin of potassic basalts; *Geochim. Cosmochim. Acta* **12** 195–208.
- Ionov D A, O' Reilly S Y and Griffin W L 1997 Volatile bearing minerals and lithophile trace elements in the upper mantle; *Chem. Geol.* **141** 153–184.
- Key R W and Gast P W 1973 The rare earth content and origin of alkali-rich basalts; *J. Geol.* **81** 653–682.
- Le Bas M J, Le Maitre R W, Strekis A and Zanettin B 1986 A chemical classification of volcanic rocks based on the total alkali silica diagrams; *J. Petrol.* **27** 745–750.
- Menzies M A and Hawkes C J 1981 *Mantle metasomatism*; Academic Press, London, 472pp.
- Moayyed M, Moazzzen M, Calagari A A, Jahangiri A and Modjarrad M 2008 Geochemistry and petrogenesis of lamprophyric dykes and the associated rocks from Eslamy peninsula, NW Iran: Implication for deep mantle metasomatism; *Chemie der Erde Geochemistry* **68** 141–154.
- Moine-Vaziri H 1985 Volcanisme tertiaire et quaternaire en Iran; *These d'Etat Univer.*, Paris-Sud, Orsay.
- Moine-Vaziri H, Khalili-marandi S H and Brousse R 1991 Importance d'un Volcanisme potassique, au miocene Superieur en Azerbaïdjan (Iran); *C.R. Acad. Sci. Paris, t.313, Serie II* 1603–1610.
- Moradian-Shahrabaky A 1997 Geochemistry, geochronology, and petrology of feldspatoid-bearing rocks in the Urumieh-Dokhtar volcanic belt, Iran; Ph.D. thesis, University of Wollongong, 411p.
- Moradian-Shahrabaky A 2007 Geological Setting and Geochronology of some alkalic and calc-alkalic rocks in western (Sary peninsula) and central (Soruk) Urmieh-Dokhtar Volcanic Belt, Iran; *Earth & Life* **2(3)** 6–24.
- Morrison G W 1980 Characteristic and tectonic setting of the shoshonitic rock association; *Lithos* **13** 97–108.
- Muller D, Rock N M S and Groves D I 1992 Geochemical discrimination between shoshonitic and potassic volcanic rocks from different tectonic setting: A pilot study; *Mineral. Petrol.* **46** 259–286.
- Muller D and Groves D I 1997 Potassic igneous rocks and associated gold-copper mineralization; *Sec. Updated*. Springer-Verlag, 242pp.
- Orejana D, Villaseca C and Paterson B A 2006 Geochemistry of pyroxenitic and hornblenditic xenoliths in alkaline lamprophyres from the Spanish Central System; *Lithos* **88** 167–196.
- Pearce J A 1983 The role of sub-continental lithosphere in magma genesis at destructive plate margins; In: *Continental Basalts and Mantle Xenoliths* (eds) Hawkesworth C J and Norry M J, Shiva, Nantwich, pp. 230–249.
- Peccerillo A 1992 Potassic and ultrapotassic rocks: Compositional characteristics, petrogenesis and geologic significance; *IUGS Episods* **15** 243–251.
- Peccerillo A and Taylor S R 1976 Geochemistry of Eocene calc-Alkaline volcanic rocks from the Kastamonu area, northern Turkey; *Contrib. Mineral. Petrol.* **58** 63–81.
- Polat A, Kerrich R and Casey J F 1997 Geochemistry of Quaternary basalts erupted along the east Anatolian and Dead Sea fault zones of southern Turkey: Implication for mantle sources; *Lithos* **40** 55–68.
- Rittman A 1933 Die geologisch beding Te evolution and differentiation des somma-vesuv Magmas; *Zeitsch fur vulkanol* **15** 8–94.
- Rock N M S 1991 *Lamprophyres*. Blackie, Glasgow, 285p.
- Rollinson H R 1993 Using geochemical data: Evaluation, Presentation, Interpretation, Longman Scientific and Technical, England, 352p.
- Roy A, Sarkar A, Jeyakumar S, Aggrawal S K, Ebihara M and Satoh H 2004 Late archaean metasomatism below eastern Indian craton. Evidence from trace element, REE geochemistry and Sr-Nd-O isotopic systematics of ultramafic dykes; *J. Earth Syst. Sci.* **113(4)** 649–665.
- Rudnick R L, McDonough W F and Chapell B W 1993 Carbonatite metasomatism in the northern Tanzanian mantle: Petrographic and geochemical characteristics; *Planet. Sci. Lett.* **114** 463–475.
- Sun S S and McDonough W F 1989 Chemical and isotopic systematic of oceanic basalts: Implication for mantle composition and processes; In: *Magmatism in the ocean basins* (eds) Saunders A D and Norry M J, *Geol. Soc. Spec. Publ.* **42** 313–345.
- Taylor S R and McLenan S M 1985 The continental crust: Its composition and evolution, Blackwell, Oxford University Press, 312pp.
- Tiepolo M, Bottazzi P, Foley S F, Orbeti R, Vannucci R and Zannetti A 2001 Fractionation of Nb and Ta from Zr and Hf at mantle depth: The role of titanian-pargasite and Kaersutite, *J. Petrol.* **42** 221–232.
- Wilson M 1989 Igneous petrogenesis a global tectonic approach; Unwin Hyman Ltd, London, 466p.